Mechanisms of sampling interstitial fluid from skin using a microneedle patch

Pradnya P. Samant[a] and Mark R. Prausnitz[a,1]

[a]School of Chemical and Biomolecular Engineering, Georgia Institute of Technology, Atlanta, GA 30332

Edited by Mark E. Davis, California Institute of Technology, Pasadena, CA, and approved March 22, 2018 (received for review September 23, 2017)

Although interstitial fluid (ISF) contains biomarkers of physiological significance and medical interest, sampling of ISF for clinical applications has made limited impact due to a lack of simple, clinically useful techniques that collect more than nanoliter volumes of ISF. This study describes experimental and theoretical analysis of ISF transport from skin using microneedle (MN) patches and demonstrates collection of >1 μL of ISF within 20 min in pig cadaver skin and living human subjects using an optimized system. MN patches containing arrays of submillimeter solid, porous, or hollow needles were used to penetrate superficial skin layers and access ISF through micropores (μpores) formed upon insertion. Experimental studies in pig skin found that ISF collection depended on transport mechanism according to the rank order diffusion < capillary action < osmosis < pressure-driven convection, under the conditions studied. These findings were in agreement with independent theoretical modeling that considered transport within skin, across the interface between skin and μpores, and within μpores to the skin surface. This analysis indicated that the rate-limiting step for ISF sampling is transport through the dermis. Based on these studies and other considerations like safety and convenience for future clinical use, we designed an MN patch prototype to sample ISF using suction as the driving force. Using this approach, we collected ISF from human volunteers and identified the presence of biomarkers in the collected ISF. In this way, sampling ISF from skin using an MN patch could enable collection of ISF for use in research and medicine.

microneedle patch | dermal interstitial fluid sampling | medical diagnostics | skin | biomarker

Diagnosis and management of disease is increasingly facilitated by measurements of biomarkers from blood, urine, saliva, and other bodily fluids. Continuing progress in biomarker discovery has enabled early diagnosis, real-time monitoring, and improved disease management (1). Blood is the most common source of biomarkers but is limited by the inability of patients to draw venous blood themselves and apprehension and sample quality of fingerstick capillary blood (2). Urine and saliva are constrained by their limited number and variable concentration of biomarkers (3, 4). Interstitial fluid (ISF) is another source of valuable and unique biomarkers but is difficult to sample from the body (5). This fluid surrounds cells and tissues throughout the body and is formed by extravasation of plasma from capillaries and modified by metabolic and other processes in the tissue (6). ISF shuttles nutrients and waste products between blood vessels and cells and is roughly a combination of serum and cellular materials.

Previous studies showed that 83% of proteins found in serum are also in ISF, but 50% of proteins in ISF are not in serum, suggesting that ISF may be a source of unique biomarkers as well as biomarkers found in blood (7, 8). Moreover, ISF may be suitable for continuous monitoring due to absence of clotting factors, as shown by commercial indwelling sensors for glucose that access ISF in the s.c. space (9). ISF is a better indicator of local tissue events as shown in tumor ISF collected from tissue biopsies (10).

Skin is the most accessible organ and therefore an attractive source of ISF containing systemic and dermatological biomarkers. ISF can currently be collected from skin using suction blisters by applying suction to skin at elevated temperature for up to 1 h to create blisters filled with ISF (11). Dermal ISF can also be sampled by implantation of tubing in skin to collect ISF biomarkers by microdialysis or open-flow microperfusion, which require local anesthesia and expert training (12, 13). The time-consuming nature of these procedures, risks to patients, and need for medical expertise and specialized equipment limit their use to basic research. Collection of ISF for more widespread research and possible future medical applications will benefit from a simpler, minimally invasive sampling method. This could enable further research into the nature and composition of ISF and the clinical utility of ISF as a body fluid for diagnostic applications.

We propose that microneedles (MNs) can be used to create micrometer-scale pathways for ISF transport out of skin across skin's outer barrier layer of stratum corneum. When coupled with a suitable driving force, an MN patch could be used to sample ISF from skin in a simple, minimally invasive manner. MNs are needle-like projections typically made from metal or polymer that measure hundreds of microns in length and thereby penetrate upper layers of skin and access skin's ISF (14, 15). MN patches have been studied extensively for drug delivery into skin and have been safe, effective, painless, and well-accepted by patients in clinical trials and other studies. However, relatively little work has been done to develop MN patches for removal of ISF from skin.

Most of skin's ISF is in dermis (16), which comprises a network of collagen and elastin fibers surrounded by extracellular matrix that limits ISF flow due to binding and tortuosity. Hence,

Significance

Diagnosis and monitoring of disease is often done by measuring biomarkers found in blood, urine, saliva, and other bodily fluids. Another rich source of biomarkers is the interstitial fluid that surrounds cells and tissues in the body, but difficulty in accessing this fluid has limited its use in research and medicine. Here, we conducted experimental studies coupled with theoretical modeling to design a patch containing microscopic needles that puncture into superficial layers of skin and thereby enable withdrawal of interstitial fluid through micropores in a simple, minimally invasive manner. This patch can help researchers access interstitial fluid to advance discovery of novel biomarkers and enable doctors to use interstitial fluid for possible future diagnosis and monitoring of disease.

Author contributions: P.P.S. and M.R.P. designed research; P.P.S. performed research; P.P.S. and M.R.P. analyzed data; and P.P.S. and M.R.P. wrote the paper.

Conflict of interest statement: M.R.P. is an inventor of patents that have been licensed to companies developing microneedle-based products, is a paid advisor to companies developing microneedle-based products, and is a founder/shareholder of companies developing microneedle-based products. This potential conflict of interest has been disclosed and is managed by Georgia Institute of Technology and Emory University.

This article is a PNAS Direct Submission.

[1]To whom correspondence should be addressed. Email: prausnitz@gatech.edu.

This article contains supporting information online at www.pnas.org/lookup/suppl/doi:10.1073/pnas.1716772115/-/DCSupplemental.

Published online April 16, 2018.

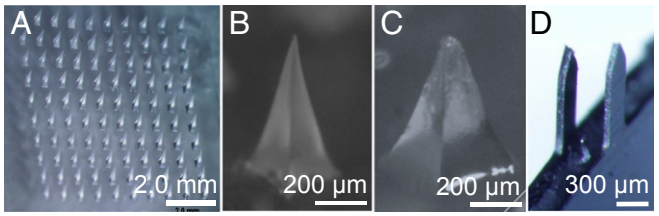

Fig. 1. ISF collection by diffusion into hydrogel MNs and skin μpores. (*A*) Representative patch containing 10 × 10 array of dried hydrogel MNs made of PVA. Magnified views of representative (*B*) dried hydrogel MN (520 μm tall) before insertion into skin, (*C*) hydrated hydrogel MN after swelling in pig skin for 12 h ex vivo, and (*D*) two stainless steel MNs (750 μm tall).

sampling ISF using MNs is a complex process involving three steps: (*i*) flow of ISF through dermis toward MNs, (*ii*) partition of ISF from dermis into MNs, and (*iii*) flow of ISF through MNs to the skin surface.

Most prior efforts to collect ISF using MNs have been limited by collection of small volumes of fluid and have emphasized demonstrations of device performance rather than systematic device analysis and design (17). Generally, diagnostic tests require at least multiple microliters of fluid for accurate measurement of analytes (18–20). Here, we used experimental and theoretical analysis to systematically evaluate ISF collection from skin by MN patches using transport mechanisms mediated by diffusion, capillary action, osmosis, and pressure-driven convection with the goal of collecting 1–10 μL of ISF within 20 min and then used the optimal design to sample ISF from human volunteers.

Results

ISF Content in Skin. To estimate the maximum amount of ISF that could be sampled from skin, we first determined that pig cadaver skin used in our studies contained 61 ± 9 wt % fluid by fully drying skin by lyophilization. It was assumed that since the cellular epidermis constitutes only ∼10% of skin volume and there are very few cells in the dermis, this figure is representative of the amount of fluid present in the interstitium, that is, ISF. This value is similar to reported values of ∼70 wt % of human dermis comprising ISF (21). Because pig cadaver skin mass was 0.25 ± 0.04 g/cm^2, this corresponds to an ISF content of ∼150 μL/cm^2 of skin. When pig skin was subjected to a large pressure (890 kPa), ISF was lost from skin through dermis at ∼1 wt %/min, such that 24 ± 6 wt % was lost after 20 min, corresponding to ISF loss of ∼60 μL/cm^2 after 20 min (*SI Appendix*, Fig. S1). This value represents the volume of mobile ISF, that is, fluid that is not otherwise bound and may provide an upper bound to the amount of ISF that could be withdrawn from skin within 20 min ex vivo, although the situation might be different in vivo due to blood flow and other effects.

ISF Collection by Diffusion into Hydrogel MNs and Micropores. One mechanism of ISF collection involves diffusion of ISF into MNs, which can be accomplished by inserting dry hydrogel MNs into skin. To study this mechanism of ISF collection, we prepared patches each containing 100 pyramidal MNs composed of cross-linked polyvinyl alcohol (PVA) (Fig. 1*A*). Upon insertion into skin, the MNs became swollen with ISF (Fig. 1 *B* and *C*). After 12 h in skin, 0.0030 μL of ISF was absorbed per MN (0.30 μL per patch). We also studied diffusion through micropores (μpores) created by puncturing and then removing metal MNs in skin (Fig. 1*D*). The volume of ISF sampled through μpores was 0.0039 μL per μpore after just 20 min. The order-of-magnitude faster ISF collection through μpores may be due to lack of transport barriers found in μpores.

ISF Collection by Capillary Flow Through Porous and Hollow MNs. The second mechanism of ISF collection we considered involves capillaries to draw ISF from skin. This can be accomplished by flow through either a network of microcapillaries in a porous MN or a single capillary in a hollow MN.

To study porous MNs, we prepared patches each containing five MNs made from paper, which were sandwiched between two stainless-steel MNs of similar dimensions for mechanical support (Fig. 2*A*). Similar paper has been characterized to have a porosity of 68% (22) and pore size of 2–10 μm (23). Upon insertion into skin, microcapillaries in the porous paper matrix absorbed 0.0033 μL per MN of ISF after 20 min (Fig. 2 *B* and *D*). To study a single capillary system, we used individual hollow MNs with a 108- to 260-μm inner diameter (Fig. 2*C*), which collected ∼0.01–0.03 μL ISF after 20 min (Fig. 2*D*). The greater ISF collection by hollow MNs may be explained in part because the MN orifice surface area was greater than the exposed surface area of porous MNs sandwiched between metal MNs.

ISF Collection by Osmotically Driven Flow via μpores. The third mechanism to sample ISF from skin uses an osmotic driving force to flow ISF from skin into μpores created by MNs. To generate an osmotic pressure gradient, we filled μpores with a solution of elevated ionic strength to drive ISF from dermis into μpores. Lacking a permselective membrane between μpores and dermis, solutes in μpores could diffuse into dermis, which accelerated the decrease of the osmotic pressure gradient over time.

A 10-MN patch coated with ∼20 μg of maltose per MN (Fig. 3*A*) was inserted into skin for 2 min to allow maltose to dissolve and was then removed. The maltose created an initial ionic strength of ∼1.17 M in the μpore, which is much higher than surrounding ISF [0.29 M (24)] and corresponds to an osmotic pressure difference of 2.2 kPa. After 20 min, 0.0056 μL of ISF was collected at the skin surface per μpore (Fig. 3*B*). In contrast, leaving MNs in skin during the 20-min ISF collection time yielded significantly less ISF (0.0006 μL per μpore), probably because MNs blocked ISF transport pathways out of skin (Fig. 3*B*).

To better maintain an osmotic driving force over time, we punctured skin for 2 min with a patch containing 10 uncoated or maltose-coated MNs and then, after removing MNs from skin, applied a 1.17 M solution of maltose to the skin surface, thereby initially filling μpores with ∼1.17 M. After 20 min, treatment using uncoated or coated MNs collected 0.024 or 0.021 μL per μpore, respectively (Fig. 3*B*), which were not significantly different from each other but were greater than treatment with coated MNs without adding maltose solution. ISF collection rate during osmotically driven transport increased steadily over the course of 60 min to a total volume of 0.070 μL per μpore (*SI Appendix*, Fig. S2). Varying the number of MNs from 10 to 50 increased ISF collected in rough proportion to the number of MNs (*SI Appendix*, Fig. S3).

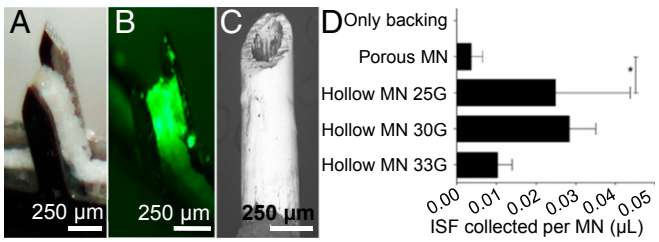

Fig. 2. ISF collection by capillary action through porous and single-capillary MNs. (*A*) Representative porous paper MN sandwiched between two stainless steel MNs for mechanical support (750 μm tall). (*B*) Representative porous paper MN that has absorbed ISF from pig skin soaked in fluorescein to facilitate ISF imaging. (*C*) Representative hollow stainless steel MN (750 μm tall) with a single hollow capillary to draw fluid out of skin. (*D*) ISF volume sampled from pig skin after 20 min: porous paper backing with no MNs (negative control), porous paper MNs, and hollow, single-capillary MNs of 33 gauge (108-μm i.d.), 30 gauge (159-μm i.d.), and 25 gauge (260-μm i.d.). Data show mean ± SD (n = 4); *P < 0.05.

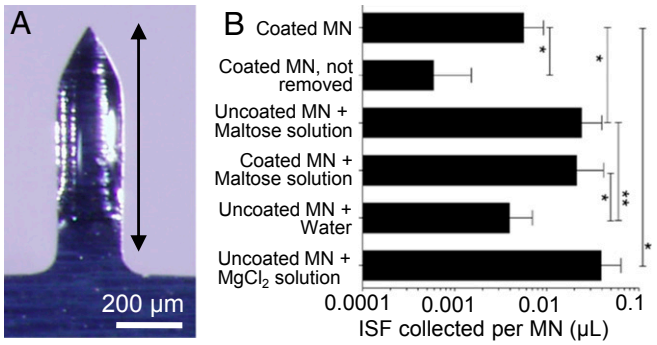

Fig. 3. ISF collection by osmosis through μpores. (*A*) Representative MN coated with maltose (bar shows coated region). (*B*) ISF volume collected from pig skin ex vivo punctured with coated and uncoated MNs followed by application of aqueous solutions of different osmotic strength for 20 min. Data show mean ± SD ($n \geq 4$); *$P < 0.05$, **$P < 0.01$.

As a control, we punctured skin with 10 uncoated MNs and then applied water to the skin surface, which provided no osmotic driving force. This collected 0.0039 μL ISF per μpore after 20 min (Fig. 3*B*), which was significantly less than that collected with an osmotic driving force and similar to ISF collection during diffusion through μpores (Fig. 2). To achieve still higher osmotic strength, we applied a solution of $MgCl_2$ with 12 M osmotic strength to skin punctured with a 10-MN patch. This collected 0.03 μL per μpore after 20 min (Fig. 3*B*). This order-of-magnitude increase in osmotic strength increased ISF collection approximately twofold. This may be explained by a faster dissipation of osmotic driving force due to faster diffusion of $MgCl_2$ away from μpores compared with maltose.

ISF Collection by Pressure-Driven Convection via μpores. A pressure difference between the dermis and skin surface can drive ISF from dermis into and through μpores. This can be accomplished by suction to create negative pressure on the skin surface at the site of μpores or by positive pressure on the skin surface at sites distant from μpores (e.g., pinch the skin), thereby creating a positive pressure in skin near μpores (*SI Appendix*, Fig. S8).

To study effects of suction on ISF collection, we punctured skin with 10-MN patches and then applied −85-kPa suction for 20 min. This produced just 0.0064 μL ISF per μpore (Fig. 4*A*). We hypothesized that suction might be collapsing μpores, so we placed skin on curved surfaces (with ∼5-mm or ∼8-mm radius of curvature) to help spread μpores open. This increased ISF collection by two orders of magnitude to 0.30 or 0.47 μL per μpore, respectively (Fig. 4*A*). Stretching skin with a strain of ∼100% on a flat surface or a curved surface produced 0.84 or 0.60 μL per μpore, respectively (Fig. 4*A*). Altogether, these data show that suction withdrew by far the most ISF from skin, but the skin surface needed to be curved and/or stretched, apparently to keep μpores open.

We next placed different kinds of absorbent paper on the skin above μpores to capture ISF collected during −85-kPa suction for 20 min. Compared with ISF collected without paper (0.71 μL per μpore), placement of thin tissue paper (Kimwipe) on skin had no significant effect (0.29 μL per μpore) (Fig. 4*B*). However, placement of gauze (∼680 μm thick) on skin reduced ISF collected by two orders of magnitude to 0.0035 μL per μpore. We hypothesized that gauze inhibited ISF collection because of its thickness and poor aqueous wettability. Plasma treating (to increase hydrophilicity) or prewetting gauze significantly increased ISF collection (0.065 or 0.12 μL per μpore, respectively; Fig. 4*B*), suggesting that surface tension played a role in ISF flow from skin to gauze. Using thinner gauze (∼150 μm thick) collected 0.17 μL per μpore, which was significantly greater than when using thick gauze (Fig. 4*B*). This suggests that gauze may have reduced the pressure drop within the skin and μpore, and that thinner gauze reduced it to a lesser extent.

We also studied effects of other MN parameters on ISF collection during suction. Varying number of MNs from 5 to 10 to 50 increased ISF collected in rough proportion to the number of MNs (*SI Appendix*, Fig. S4). Increasing MN length between 250–750 μm on 10-MN patches showed a trend of less ISF collected as MN length increased, but this was not statistically significant (*SI Appendix*, Fig. S5). Use of patches with polymer MNs that tapered from a wide base (which was needed for mechanical strength of polymer MNs) was less effective compared with thin metal MNs used in the rest of this study (*SI Appendix*, Fig. S6), probably because polymer MNs did not insert as deeply into skin (15). Finally, using three different MN designs, we compared curved skin to stretched skin and found they each provided similar ISF collection under the conditions used (*SI Appendix*, Fig. S7).

Finally, we generated positive pressure in skin by pinching to drive ISF out of the skin (*SI Appendix*, section S1.8). After applying a 10-MN patch and then administering a positive pressure (estimated to be 25 kPa inside skin below μpores) for 20 min, 0.16 μL ISF per μpore was collected (Fig. 4*C*). We also found that the amount of ISF collected increased linearly over time when either positive or negative pressure was applied (Fig. 4*C*).

ISF Collection from the Skin of Human Volunteers. Guided by the above findings, we used 50-MN stainless steel patches to create μpores followed by suction for 20 min (*SI Appendix*, Fig. S9). This collected 2.3 ± 2.1 μL ISF per person based on 17 separate ISF collections from six different volunteers. Determination of ISF volume assumed that sodium concentration in human ISF is constant at 135 mmol/L, although this value may vary by ∼10% in healthy individuals (25). The collected fluid was clear, with little or no evidence of blood. Since ISF transport occurred through μpores and not the entire stratum corneum, ISF appeared as droplets on the skin surface (Fig. 5*C*). ISF flow rate was not quantified as a function of time, but our observation was that ISF first appeared on the skin surface after ∼30 s of vacuum and then steadily increased over time. There was spatial heterogeneity of ISF collection within each array of 50 μpores, where some μpores produced visible amounts of ISF and others

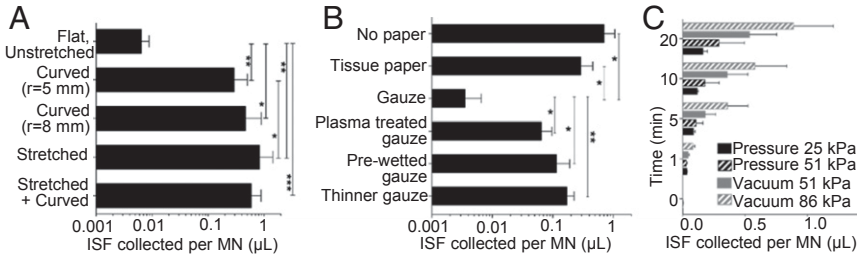

Fig. 4. ISF collection by pressure-driven convective flow through μpores. ISF collected from MN-punctured pig skin ex vivo after 20 min of suction (−85 kPa) (*A*) for skin under different degrees of tension and (*B*) for skin covered by different absorbent papers. (*C*) ISF collected from pig skin ex vivo after different durations and levels of suction and positive pressure applied to skin. Data show mean ± SD ($n \geq 3$); *$P < 0.05$, **$P < 0.01$, ***$P < 0.001$.

did not. Mild erythema was observed at the skin site, which resolved completely within 24 h (Fig. 5). In a few cases, 15–20 faint, pink, submillimeter spots were visible at sites where individual MNs had penetrated skin and disappeared within 24 h. The erythema was of possible cosmetic significance, but not clinically meaningful. Volunteers generally reported little or no pain associated with the procedure. No adverse events were recorded, and overall the procedure was well-tolerated.

Collected ISF from 11 subjects was analyzed for glucose and total protein content as representative biomarkers. The concentration of glucose in ISF was 91 ± 11 mg/dL and total protein concentration was 90 ± 21 mg/mL (*SI Appendix*, Fig. S10*A*). We also collected companion plasma samples from the subjects from fingerstick capillary blood. The concentration of glucose in plasma was 100 ± 25 mg/dL and total protein concentration was 105 ± 26 mg/mL (*SI Appendix*, Fig. S10*B*), which is comparable to the concentrations in ISF (Student's t test, $P > 0.05$).

Theoretical Model to Predict ISF Collection Rates. To better understand underlying mechanisms governing ISF transport through skin, MNs, and μpores, we modeled ISF transport in the scenarios explored in this study. Our goal was to predict ISF collection rates in each scenario and identify rate-limiting steps to enable improved ISF collection. The theoretical modeling considered three steps in the transport process: transport through skin to the MN (or μpore) interface, transport/partitioning across the skin–MN interface, and transport through or within MN. To provide independent predictions of ISF behavior in skin, theoretical predictions were based on first-principle models using parameter values that were measured, independently calculated, or adapted from literature; there were no fitted parameters. Predicted values match experimentally observed values reasonably well, especially given the simplified theoretical analysis with no fitted parameters, and are often within the error bars of the data (*SI Appendix*, section S2.6).

ISF collection by hydrogel MNs was modeled as ISF diffusion through dermis and then, upon partitioning into the hydrogel, diffusion through the hydrogel matrix (*SI Appendix*, section S2.1). As ISF diffusivity in dermis is greater than in PVA hydrogel used in this study, diffusion of ISF through hydrogel was rate-limiting and significantly constrained ISF collection rates (*SI Appendix*, Fig. S11). Using a different hydrogel with higher ISF diffusivity [e.g., as described by Chang et al. (26)] can increase rates of ISF uptake. However, once ISF diffusivity in hydrogel approaches and exceeds that in dermis, dermis becomes a rate-limiting step and further improvements to hydrogel permeability have diminishing impact. Similarly, ISF collection through μpores is limited by low ISF diffusivity in dermis, so dermis is a rate-limiting step (*SI Appendix*, section S2.2).

ISF collection by capillary flow into porous and hollow MNs involves rapid convective flow within MNs, effectively making MNs a sink, which maximizes the concentration gradient in nearby dermis (*SI Appendix*, section S2.3). The rate-limiting step is exclusively in dermis, which makes ISF collection faster than in the case of hydrogel MNs or μpores where ISF diffusivity in the MN/μpore can be fast but is still a barrier (*SI Appendix*, Fig. S13). Although changes in MN design to increase capillary forces may not increase ISF uptake further, ISF uptake scales directly with area of MN–dermis contact. This explains why ISF collected by hollow MNs was greater than porous MNs, because the surface area of the hollow MN orifice was larger than that of porous MNs.

ISF collection by osmotically driven flow through μpores provides a transient convective driving force in the μpore and dermis (*SI Appendix*, section S2.4). As osmolyte (e.g., maltose) diffuses from the μpore, a gradient of osmolyte is formed in surrounding dermis (*SI Appendix*, Fig. S14). The resulting osmotic pressure gradient within dermis drives ISF convectively to the μpore. This driving force for ISF convection in dermis differs from ISF collection by hydrogel or capillary MNs, which rely on ISF diffusion in dermis.

However, osmotically driven convection was transient because over time osmolyte diffuses away from the μpore, such that the osmotic pressure gradient decays to zero. To increase ISF collection, osmotic driving force could be increased by increasing osmolyte concentration and could be sustained longer by decreasing diffusivity of osmolyte in dermis. Thus, high molar water solubility and high molecular weight are good, and perhaps competing, properties of optimal osmolyte.

ISF collection by pressure-driven convection through μpores creates the largest pressure drop across the rate-limiting barrier of dermis to drive ISF into μpores (*SI Appendix*, section S2.5). Whether by vacuum on the skin surface or positive pressure applied by "pinching," pressure drop is inherently focused on regions with greatest flow resistance in dermis. While the initial osmotic pressure gradient was 49 kPa/mm, it dropped almost to zero after 20 min. Direct application of vacuum or pressure achieved larger pressure gradients (131 kPa/mm or 77 kPa/mm, respectively) that remained constant. ISF collection could be further increased by increasing vacuum or applied pressure but would be limited by pain and skin damage (27).

Discussion

To improve on invasive and time-consuming methods to sample dermal ISF currently available (11, 12), prior studies developed hollow MNs to withdraw ISF by capillary action (28, 29), solid hydrogel MNs that swell with ISF (14, 26, 30, 31), and solid MNs to puncture μpores in skin for ISF collection under suction (32). These prior approaches have generally been limited by small sampling volumes (e.g., <1 μL) (17). Other MN designs have selectively bound targeted biomarkers to MNs in skin (33, 34), which requires customized MNs and procedures to elute biomarkers off MNs for analysis. Here, we systematically evaluated mechanisms of ISF collection from skin with the goal of a minimally invasive, simple-to-administer MN-based system to sample >1 μL ISF from skin within 20 min. This volume suffices for many assays of clinical interest like sodium, glucose, troponin, and cholesterol (18–20). A 20-min sampling time is compatible with a typical doctor's visit and patient-administered testing at home. Theoretical modeling identified rate-limiting steps to ISF flow.

Analysis of ISF Sampling Methods. Hydrogel MNs sampled the smallest ISF volume, which was limited by diffusion in dermis and MNs. As ISF diffusivity in hydrogel increases, the rate-limiting step shifts from MN to dermis. However, even when ISF diffusivity in MNs (or μpores) approaches that of free self-diffusion of water, diffusion through dermis remains rate-limiting. ISF sampling rates are constrained because of diffusion without convective forces.

Capillary action increased ISF flow rate. Due to convective transport, flow through capillaries of porous or hollow MNs was not rate-limiting, leaving diffusion through dermis as the limiting barrier. Further optimization of MN design should increase MN–dermis interfacial area, which scales directly with ISF collection rate.

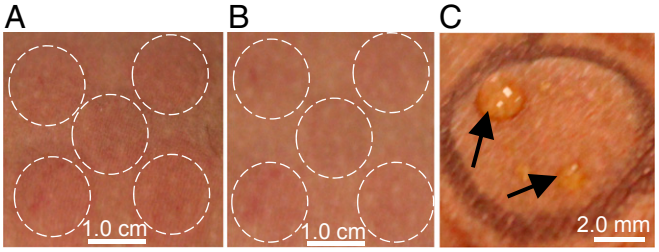

Fig. 5. ISF collection from human volunteers by suction through μpores. Representative images of skin (*A*) immediately after suction show faint erythema and no evidence of edema or bleeding (dashed white circles identify sites of ISF collection through 50 μpores) and (*B*) 24 h after ISF collection show resolution of erythema. (*C*) Representative image showing ISF droplets on skin surface after collection by suction through μpores.

ISF collection rate using osmosis increased by an order of magnitude. Diffusion of osmolyte from μpores into dermis generates an osmotic pressure gradient that drives convective flow in the rate-limiting barrier of dermis. MNs coated with osmolyte were less effective to collect ISF probably because the small amount of osmolyte delivered into skin diffused away quickly. A reservoir of osmolyte on skin surface helped maintain high osmotic strength in μpores and dermis, even as osmolyte diffused away, thereby increasing ISF collection. Flow of ISF into μpores was governed by two transient, competing parameters: osmotic pressure generated by osmolyte diffusion into dermis near μpores (increasing osmotic pressure) and osmolyte diffusion away from μpores in dermis (decreasing osmotic pressure). ISF collection could be increased by increasing number of μpores, increasing osmotic pressure by increasing osmolyte concentration, or decreasing speed of osmotic pressure gradient decay by slowing osmolyte diffusion into dermis.

While transient convection in dermis due to osmotic pressure gradients improved ISF collection, continuous application of pressure gradient across dermis via pressure or suction maximized ISF sampling. Effective ISF collection using suction required stretched/curved skin, which probably forced μpores open during vacuum application. ISF collection on the skin surface also depended on material covering the μpores to collect ISF. A thin hydrophilic cover did not interfere with pressure drop in skin and allowed ISF to readily flow out of the μpore. ISF flow varied linearly with time and pressure and was limited by flow conductivity of dermis and applied pressure gradient. During suction, maximum possible pressure drop is 101 kPa (i.e., 1 atm), and both positive and negative pressure are further limited by sensitivity of skin tissue to pressure. Even with these constraints, ISF collection achieved the target of >1 μL within 20 min in pig skin ex vivo and human volunteers. Glucose and protein were each found at similar levels in ISF and plasma but did not vary sufficiently in the healthy human volunteers to establish correlations. Previous studies have shown correlation of glucose levels in ISF to plasma (25, 35, 36).

Compared with living skin, ex vivo studies may underpredict ISF collection rates due to blood perfusion, lymph flow, and fluid dynamics in skin and overpredict due to physiological osmotic gradients in dermis. Future research should address limitations of the study, such as increasing ISF collection rate to produce more ISF in less time, reducing variability in amount of ISF collected probably due to interpersonal and time-dependent differences is tissue hydration and other properties, and enabling ISF collection using a smaller and simpler device compared the bulky pump used here.

MN Treatment Acceptability, Safety, and Impact. ISF is a rich source of biomarkers that has received limited attention for lack of good collection methods. ISF can be an alternative to blood sampling; many proteins of medical interest found in blood were also in ISF from suction blisters (7, 8). Skin proteins, like dermicidin and dermokine (37, 38), were preferentially found in ISF, suggesting that it could provide biomarkers not readily found in blood (8). ISF is also valuable to dermatological pharmacokinetics in skin (12).

ISF sampling is currently done using suction blisters, microdialysis, and microperfusion, which require expert technique, cause tissue trauma, and are costly and time-consuming (11–13). ISF collection using methods described here is minimally invasive, causes little or no pain, is simple to administer, is well-tolerated by skin, and can collect useful amounts of ISF relatively quickly. Previous studies in human volunteers have shown that MNs like those used here (but without collecting ISF) create μpores that close and cause mild erythema that resolves within hours (39, 40).

Here, MNs were combined with suction to withdraw ISF from human volunteers. This combined procedure caused only mild erythema, primarily associated with suction, and resolved within 24 h. Suction is well-accepted and safely applied to skin in existing procedures such as negative-pressure wound therapy, suction electrodes for ECG recording, and cupping in traditional Chinese medicine (41, 42). Suction, though mild, may be contraindicated in certain people, such as infants or the elderly, who may have sensitive skin. We expect that mild, transient erythema, will be acceptable for clinical applications of MNs. Although skin infections have not been reported due to MNs in other contexts (43), formation of μpores may not be appropriate in certain populations, such as those with weak immune systems or certain skin diseases (44). Safety of ISF collection using MNs needs additional study.

This study should motivate further investigation of ISF composition compared with other body fluids such as plasma and in different populations and identification of clinically valuable biomarkers in ISF. We believe that MN-based ISF collection can facilitate such studies and, in the future, make ISF routinely accessible for medical research, diagnosis, and monitoring. Applications could include continuous analyte measurement for monitoring concentration of glucose or drugs with narrow therapeutic index, detection and typing of local skin diseases such as skin cancer, or monitoring stress levels in susceptible populations like military personnel. Because ISF does not clot, it might be sampled continuously by a wearable system, possibly operated by patients themselves. A versatile method of ISF collection suitable for widespread use is required to enable these applications.

Conclusion

ISF is a unique bodily fluid of great potential interest as a source of biomarkers but has received little prior attention due largely to a lack of straightforward methods to collect ISF from skin. This study found that ISF can be collected from skin using mechanisms that provide diffusive and/or convective driving forces with effectiveness in the following rank order: diffusion < capillary action < osmosis < applied pressure/suction. As determined by theoretical modeling (with no fitted parameters), ISF transport in skin was rate-limiting, such that methods providing convective forces in dermis (i.e., osmosis and applied pressure/suction) collected the most ISF. ISF collection by MNs combined with suction was well-tolerated in human volunteers and produced ISF in sufficient quantity to identify biomarkers. Mechanistic understanding, MN device prototype development, and successful demonstration in human volunteers shown here may enable ISF collection by MN patch to become a platform technology for diverse applications in medical research, diagnostics, and monitoring.

Materials and Methods

MN Fabrication. Hydrogel MNs were prepared by casting an aqueous solution of PVA onto silicone molds in the inverse shape of MN arrays, followed by PVA cross-linking at elevated temperature and drying overnight (Fig. 1 *A* and *B*). Metal MNs were fabricated by chemically etching stainless-steel sheets. The 10-MN arrays were made by adhering two planar arrays of solid metal MNs with a spacer (Fig. 1*D*). To fabricate porous MNs, sheets of filter paper were laser-cut using metal MNs as a protective mask. This yielded paper MNs which were sandwiched between two metal MN arrays for mechanical strength (Fig. 2*A*). Hollow MNs were made by shortening and rebeveling hypodermic needles using a rotary tool (Fig. 2*C*). Coated MNs were made by dipping solid metal MNs into an aqueous solution of maltose (Fig. 3*A*). See *SI Appendix* for details.

Measurement of ISF Content in Skin. ISF content in skin was measured by weight loss of pig ear skin after lyophilization. ISF that could be removed from skin was measured by weight loss after applying pressure to pig skin over time. See *SI Appendix* for details.

Measurement of ISF Collected from Skin During MN-Based Protocols. Pig ear skin was equilibrated overnight with fluorescein solution. Pig ear skin is similar in anatomy to human skin and is widely used to study transdermal delivery and skin physiology (45). Hydrogel MN arrays were inserted into skin for 12 h to allow MNs to extract ISF. μpores were created with a 10-MN patch inserted and removed immediately from pig skin. Fluid on skin surface was wiped off after 20 min for analysis. Porous MN arrays were inserted and left

in skin for 20 min to collect ISF. Hollow MNs attached to a syringe were inserted and left in pig skin for 20 min to collect ISF. For osmosis, maltose from a coated MN patch was allowed to dissolve to create μpores filled with maltose solution. To fill μpores with osmolyte solution, maltose solution was pipetted onto μpores created with plain/coated 10-MN arrays. The system was left for 20 min to allow μpores to take up ISF. Fluid on the skin surface was collected after 20 min with tissue paper. To evaluate ISF collected by pressure-driven convection, μpores were created in skin with a 10-MN array. Suction was applied with a vacuum pump over μpores. To make a curvature on the skin surface, a disk was placed under the skin surface. To stretch out skin, the ends of the skin piece were stretched by hand and secured to a wooden board. Suction was applied over the μpores for a designated amount of time and ISF on the surface was collected by tissue paper. For MNs utilizing pressure, μpores were created in skin. The skin piece was folded in half with the pores at the apex and placed horizontally on the bench top. Pressure was applied over the skin surface using iron weights for a designated amount of time. To elute all ISF solutes absorbed using MN patches, the MNs or the tissue paper or gauze used to collect ISF was soaked in deionized (DI) water for 24 h. ISF collected was measured by measuring the amount of fluorescein in the sample and normalizing against fluorescein concentration in skin (i.e., 1 mg/mL). All reported fluxes and flow rates were averaged over the period of ISF collection (usually 20 min).

ISF was collected from human volunteers over 20 min by applying 34- to 68-kPa suction over μpores created by a sterile 10-MN patch. ISF on skin surface was collected using sterile gauze pads, subsequently soaked in DI water to recover ISF. All volunteers provided informed consent. This study was approved by Georgia Tech Institutional Review Board. ISF volume was determined by sodium ion concentration normalized to its concentration in standard ISF. Glucose and protein were measured using glucose and micro-BCA assays, respectively. See *SI Appendix* for details.

ACKNOWLEDGMENTS. We thank D. Bondy for administrative support; J. C. Joyce, J. W. Lee, W. Pewin, A. Romanyuk, and A. Tadros for help fabricating patches; C. Massaro, K. Nueberger, J. Palacios, Z. Schneiderman, and A. Yucesoy for assistance in experiments; and S. Henry and D. V. McAllister for help developing human protocols.

1. Baker M (2005) In biomarkers we trust? *Nat Biotechnol* 23:297–304.
2. Bond MM, Richards-Kortum RR (2015) Drop-to-drop variation in the cellular components of fingerprick blood: Implications for point-of-care diagnostic development. *Am J Clin Pathol* 144:885–894.
3. Nunes LA, Mussavira S, Bindhu OS (2015) Clinical and diagnostic utility of saliva as a non-invasive diagnostic fluid: A systematic review. *Biochem Med (Zagreb)* 25:177–192.
4. Slupsky CM, et al. (2007) Investigations of the effects of gender, diurnal variation, and age in human urinary metabolomic profiles. *Anal Chem* 79:6995–7004.
5. Fogh-Andersen N, Altura BM, Altura BT, Siggaard-Andersen O (1995) Composition of interstitial fluid. *Clin Chem* 41:1522–1525.
6. Scallan J, Huxley VH, Korthuis RJ (2010) *Capillary Fluid Exchange: Regulations, Function and Pathology*, Colloquium Lectures on Integrated Systems Physiology–From Molecules to Function, ed Granger DN, Granger JP (Morgan & Claypool, San Rafael, CA), pp 1–33.
7. Kool J, et al. (2007) Suction blister fluid as potential body fluid for biomarker proteins. *Proteomics* 7:3638–3650.
8. Müller AC, et al. (2012) A comparative proteomic study of human skin suction blister fluid from healthy individuals using immunodepletion and iTRAQ labeling. *J Proteome Res* 11:3715–3727.
9. Luijf YM, et al.; AP@home consortium (2013) Accuracy and reliability of continuous glucose monitoring systems: A head-to-head comparison. *Diabetes Technol Ther* 15: 722–727.
10. Gromov P, et al. (2013) Tumor interstitial fluid—A treasure trove of cancer biomarkers. *Biochim Biophys Acta* 1834:2259–2270.
11. Kiistala U (1968) Suction blister device for separation of viable epidermis from dermis. *J Invest Dermatol* 50:129–137.
12. Krogstad AL, Jansson PA, Gisslén P, Lönnroth P (1996) Microdialysis methodology for the measurement of dermal interstitial fluid in humans. *Br J Dermatol* 134:1005–1012.
13. Bodenlenz M, et al. (2017) Open flow microperfusion as a dermal pharmacokinetic approach to evaluate topical bioequivalence. *Clin Pharmacokinet* 56:91–98, and erratum (2017) 56:99.
14. Donnelly RF, et al. (2014) Microneedle-mediated minimally invasive patient monitoring. *Ther Drug Monit* 36:10–17.
15. Prausnitz MR (2017) Engineering microneedle patches for vaccination and drug delivery to skin. *Annu Rev Chem Biomol Eng* 8:177–200.
16. Amirlak B (2013) Skin anatomy. Available at https://emedicine.medscape.com/article/1294744-overview.
17. Miller PR, Narayan RJ, Polsky R (2016) Microneedle-based sensors for medical diagnosis. *J Mater Chem B* 4:1379–1383.
18. Parikh P, Mochari H, Mosca L (2009) Clinical utility of a fingerstick technology to identify individuals with abnormal blood lipids and high-sensitivity C-reactive protein levels. *Am J Health Promot* 23:279–282.
19. Garg SK, et al. (1999) Correlation of fingerstick blood glucose measurements with GlucoWatch biographer glucose results in young subjects with type 1 diabetes. *Diabetes Care* 22:1708–1714.
20. Loewenstein D, Stake C, Cichon M (2013) Assessment of using fingerstick blood sample with i-STAT point-of-care device for cardiac troponin I assay. *Am J Emerg Med* 31:1236–1239.
21. Aukland K, Nicolaysen G (1981) Interstitial fluid volume: Local regulatory mechanisms. *Physiol Rev* 61:556–643.
22. Wang J, et al. (2014) Hydrophobic sol-gel channel patterning strategies for paper-based microfluidics. *Lab Chip* 14:691–695.
23. Gribble CM, et al. (2011) Porometry, porosimetry, image analysis and void network modelling in the study of the pore-level properties of filters. *Chem Eng Sci* 66: 3701–3709.
24. Pierre Agache PH (2004) *Measuring the Skin* (Springer, Berlin), 784 p.
25. Sieg A, Guy RH, Delgado-Charro MB (2004) Noninvasive glucose monitoring by reverse iontophoresis in vivo: Application of the internal standard concept. *Clin Chem* 50:1383–1390.
26. Chang H, et al. (2017) A swellable microneedle patch to rapidly extract skin interstitial fluid for timely metabolic analysis. *Adv Mater* 29:1702243.
27. Santos D, Carline T, Richmond R, Abboud RJ (2003) A review of the effects of external pressure on skin blood flow. *Foot* 13:185–189.
28. Miller PR, et al. (2012) Hollow microneedle-based sensor for multiplexed transdermal electrochemical sensing. *J Vis Exp* e4067.
29. Mukerjee EV, Collins SD, Isseroff RR, Smith RL (2004) Microneedle array for transdermal biological fluid extraction and in situ analysis. *Sens Actuators A Phys* 114: 267–275.
30. Caffarel-Salvador E, et al. (2015) Hydrogel-forming microneedle arrays allow detection of drugs and glucose: Potential for use in diagnosis and therapeutic drug monitoring. *PLoS One* 10:e0145644.
31. Romanyuk AV, et al. (2014) Collection of analytes from microneedle patches. *Anal Chem* 86:10520–10523.
32. Wang PM, Cornwell M, Prausnitz MR (2005) Minimally invasive extraction of dermal interstitial fluid for glucose monitoring using microneedles. *Diabetes Technol Ther* 7: 131–141.
33. Corrie SR, et al. (2010) Surface-modified microprojection arrays for intradermal biomarker capture, with low non-specific protein binding. *Lab Chip* 10:2655–2658.
34. Muller DA, Corrie SR, Coffey J, Young PR, Kendall MA (2012) Surface modified microprojection arrays for the selective extraction of the dengue virus NS1 protein as a marker for disease. *Anal Chem* 84:3262–3268.
35. Jina A, et al. (2014) Design, development, and evaluation of a novel microneedle array-based continuous glucose monitor. *J Diabetes Sci Technol* 8:483–487.
36. Bolinder J, Ungerstedt U, Arner P (1992) Microdialysis measurement of the absolute glucose concentration in subcutaneous adipose tissue allowing glucose monitoring in diabetic patients. *Diabetologia* 35:1177–1180.
37. Broccardo CJ, Mahaffey SB, Strand M, Reisdorph NA, Leung DY (2009) Peeling off the layers: Skin taping and a novel proteomics approach to study atopic dermatitis. *J Allergy Clin Immunol* 124:1113–1115.e11.
38. Matsui T, et al. (2004) Identification of novel keratinocyte-secreted peptides dermokine-α/-β and a new stratified epithelium-secreted protein gene complex on human chromosome 19q13.1. *Genomics* 84:384–397.
39. Arya J, et al. (2017) Tolerability, usability and acceptability of dissolving microneedle patch administration in human subjects. *Biomaterials* 128:1–7.
40. Bal S, et al. (2010) In vivo visualization of microneedle conduits in human skin using laser scanning microscopy. *Laser Phys Lett* 7:242–246.
41. Cao H, Li X, Liu J (2012) An updated review of the efficacy of cupping therapy. *PLoS One* 7:e31793.
42. Apelqvist J, et al. (2017) EWMA document: Negative pressure wound therapy. *J Wound Care* 26(Suppl 3):S1–S154.
43. Prausnitz MR, Mikszta JA, Cormier M, Andrianov AK (2009) Microneedle-based vaccines. *Vaccines for Pandemic Influenza*, eds Compans RW, Orenstein WA (Springer, New York), pp 370–393.
44. Kelchen MN, et al. (2016) Micropore closure kinetics are delayed following microneedle insertion in elderly subjects. *J Control Release* 225:294–300.
45. Abd E, et al. (2016) Skin models for the testing of transdermal drugs. *Clin Pharmacol* 8:163–176.